Risk of groundwater contamination widely underestimated because of fast flow into aquifers

Andreas Hartmann[a,b,1], Scott Jasechko[c], Tom Gleeson[d], Yoshihide Wada[e,f], Bartolomé Andreo[g], Juan Antonio Barberá[g], Heike Brielmann[h], Lhoussaine Bouchaou[i,j], Jean-Baptiste Charlier[k,l], W. George Darling[m], Maria Filippini[n], Jakob Garvelmann[o,p], Nico Goldscheider[q], Martin Kralik[r], Harald Kunstmann[o,s], Bernard Ladouche[k,l], Jens Lange[t], Giorgia Lucianetti[u], José Francisco Martín[g], Matías Mudarra[g], Damián Sánchez[g], Christine Stumpp[v], Eleni Zagana[w], and Thorsten Wagener[b,x,y]

[a]Hydrological Modeling and Water Resources, University of Freiburg, D-79098 Freiburg, Germany; [b]Department of Civil Engineering, University of Bristol, BS8 1TR, Bristol, United Kingdom; [c]Bren School of Environmental Science and Management, University of California Santa Barbara, Santa Barbara, CA 93117; [d]Department of Civil Engineering and School of Earth and Ocean Sciences, University of Victoria, Victoria, BC V8P 5C2, Canada; [e]International Institute for Applied Systems Analysis, A-2361 Laxenburg, Austria; [f]Department of Physical Geography, Utrecht University, 3584 CS Utrecht, The Netherlands; [g]Department of Geology and Centre of Hydrogeology at the University of Malaga, 29071, Malaga, Spain; [h]Environment Agency Austria, Groundwater Unit, Spittelauer Laende 5, A-1090 Vienna, Austria; [i]Laboratory of Applied Geology and Geo- Environment, Ibn Zohr University, BP 8106 Agadir, Morocco; [j]International Water Research Institute, Mohammed VI Polytechnic University, Ben Guerir 43150, Morocco; [k]BRGM, University of Montpellier, F-34000 Montpellier, France; [l]G-eau, INRAE, CIRAD, IRD, AgroParisTech, Supagro, BRGM, F-34196 Montpellier, France; [m]British Geological Survey, Wallingford OX10 8ED, United Kingdom; [n]Department of Biological Geological and Environmental Sciences, Alma Mater Studiorum–University of Bologna, 40127, Bologna, Italy; [o]Institute of Meteorology and Climate Research, Karlsruhe Institute of Technology, Campus Alpin, D-82467 Garmisch-Partenkirchen, Germany; [p]boden & grundwasser Allgäu GmbH, D-87527 Sonthofen, Germany; [q]Institute of Applied Geosciences, Karlsruhe Institute of Technology, D-76131 Karlsruhe, Germany; [r]Department of Environmental Geosciences, Center for Microbiology and Environmental Systems Science, University of Vienna, 1090 Vienna, Austria; [s]Institute of Geography, University of Augsburg, D-86135 Augsburg, Germany; [t]Hydrology, University of Freiburg, D-79098 Freiburg,Germany; [u]Department of Sciences, Roma Tre University, 00146 Rome, Italy; [v]Institute for Soil Physics and Rural Water Management, Department of Water, Atmosphere and Environment, University of Natural Resources and Life Sciences, A-1190 Vienna, Austria; [w]Laboratory of Hydrogeology, Department of Geology, University of Patras, 26500 Rion Patras, Greece; [x]Cabot Institute, University of Bristol, BS8 1UH, Bristol, United Kingdom; and [y]Institute for Environmental Science and Geography, University of Potsdam, D-14476, Potsdam, Germany

Groundwater pollution threatens human and ecosystem health in many regions around the globe. Fast flow to the groundwater through focused recharge is known to transmit short-lived pollutants into carbonate aquifers, endangering the quality of groundwaters where one quarter of the world's population lives. However, the large-scale impact of such focused recharge on groundwater quality remains poorly understood. Here, we apply a continental-scale model to quantify the risk of groundwater contamination by degradable pollutants through focused recharge in the carbonate rock regions of Europe, North Africa, and the Middle East. We show that focused recharge is the primary reason for widespread rapid transport of contaminants to the groundwater. Where it occurs, the concentration of pollutants in groundwater recharge that have not yet degraded increases from <1% to around 20 to 50% of their concentrations during infiltration. Assuming realistic application rates, our simulations show that degradable pollutants like glyphosate can exceed their permissible concentrations by 3 to 19 times when reaching the groundwater. Our results are supported by independent estimates of young water fractions at 78 carbonate rock springs over Europe and a dataset of observed glyphosate concentrations in the groundwater. They imply that in times of continuing and increasing industrial and agricultural productivity, focused recharge may result in an underestimated and widespread risk to usable groundwater volumes.

groundwater | recharge | contamination

Clean water is essential for nature and society (1), but pollution can reduce available drinking water and threaten ecosystem services (2). Large-scale studies on water security so far have mainly focused on water quantity rather than water quality (3). Local-scale studies have shown that focused recharge is a dominant driver of groundwater pollution in carbonate rock regions (4, 5). Chemical weathering of carbonate rock (in this context, often referred to as karstification) results in karst environments with enhanced porosity and permeability (6, 7). Depending on the strength of karstification, this can substantially increase the potential for focused recharge (8). Fast flow through fractures and macropores in the soil can mobilize pollutants, even though some have been considered "nonleachable" owing to their strong adsorption onto colloids and sediment surfaces in the soil or due to fast degradation times (9). Consequently, in addition to the dangers of more persistent pollutants like nitrate (10), focused recharge may cause unexpected groundwater quality deterioration in regions where agriculture relies on degradable fertilizers and pesticides (11, 12). Although agriculture occupies around 40% of ice-free lands (13), as of yet, there are no continental-scale assessments of the impact of focused recharge and degradable pollutants on groundwater quality.

Significance

Clean groundwater is essential for water supply in many regions of the world. Fast flow to the groundwater through enlarged cracks and fissures, which is known to transmit short-lived pollutants into the groundwater, is often neglected in large-scale studies. We quantify the rapid transport of pollutants by fast flow into the carbonate rock groundwater storage in Europe, North Africa, and the Middle East. We show that, through rapid transport, up to 50% of infiltrating pollutants may still reach the groundwater table, which is substantially more than estimated when fast transport is neglected. These results imply that the contamination risk of usable groundwater storages is much larger than expected where fast flow to the groundwater occurs.

This work estimates the risk of groundwater contamination by the rapid transport of short-lived pollutants to the groundwater through focused recharge in karst terrane. We do this by comparing the travel times of water from the surface to the subsurface with the degradation times of typical degradable pollutants. Our research domain is the carbonate rock regions of Europe, North Africa, and the Middle East, collectively home to around half a billion people and provider of up to half of the national water supplies in these regions (14). Globally, 10 to 25% of the world's population are estimated to largely or entirely depend on groundwater from carbonate rock aquifers (15, 16). In carbonate rock regions, focused recharge occurs as fast flow from the surface to the groundwater via localized infiltration from local depressions into enlarged cracks or fissures (17). During rainfall events, this characteristic of karstified carbonate rock allows large volumes of water to enter the subsurface (14, 18) and can transport surface-borne pollutants—dissolved or attached to suspended sediments—to the groundwater over short time scales (i.e., within days or weeks) (19, 20). We define the rapid recharge fractions that correspond to these short time scales as the volumetric fractions of recharge that reach the groundwater within predefined transit times. We derive the rapid recharge fractions by simulating transit time distributions with a state-of-the-art continental model (18, 21) that accounts for focused recharge processes in carbonate rock regions. For analysis, our simulation domain is divided into four regions: humid, mountains, Mediterranean, and deserts (see model description in *Materials and Methods*).

In this study, we define the risk of groundwater contamination by the probability of different short-lived pollutants reaching the groundwater before degradation (i.e., the probability of degradation times exceeding the transport time to the groundwater). We simulate rapid recharge fractions with different transit times using the half-lives and survival times of degradable pollutants derived at field conditions in the soil (pH: ~5 to 7, temperature: 5 to 30 °C, unsaturated/aerobic conditions, no photo-degradation). They range from half-lives and survival times of 5 d, representing immediate transfer after rainfall events, to 90 d, representing transfer within the same season (*SI Appendix*, Table S4). To elaborate on our findings, we focus on three example pollutants, a veterinary pharmaceutical common in manure [Salinomycin, 10 d half-lives (11)], a degradable pesticide [glyphosate, 25 d half-lives (22)], and a common pathogen [*Escherichia coli*, 60 d survival time (12)]. We quantify the influence of focused recharge processes on fast transit to the groundwater by repeating the simulations with only diffuse recharge considered (see model description in *Materials and Methods*), which is how presently available large-scale models represent groundwater recharge (14). To explore the impact of climate, we compare simulated rapid recharge fractions with climate descriptors such as mean annual precipitation and temperature, aridity index (defined here as long-term ratio of precipitation to potential evapotranspiration), mean annual number of rainfall events, and mean annual duration of snow cover. We evaluate the consistency of our model with independently derived young water fractions—the fraction of water less than 60 to 90 d old (23, 24)—corrected for precipitation seasonality (25) at the most reliable 78 out of 119 carbonate rock springs datasets (26) across our simulation domain (see simulation of transit times in *Materials and Methods*) and with a dataset of >2,500 groundwater samples that were analyzed for glyphosate abundance and concentration inside and outside the karst regions of the United States (27, 28).

Results

Continental-Scale Estimation of Rapid Recharge Fractions. Our simulations indicate that the share of focused recharge that transits to the groundwater within one season (90 d, Fig. 1*A*) is up to $77 \pm 14\%$ in the Mediterranean, $50 \pm 17\%$ in the mountain regions, $46 \pm 11\%$ in the desert regions, and $41 \pm 11\%$ in the humid

regions. Our comparison of the simulated rapid recharge fractions with the observed young water fractions from the carbonate rock springs shows significant correlation ($r = 0.83$, $P \le 0.001$), though with some tendency to overestimate young water fractions for some springs in humid and mountain regions where estimated young water fractions are low. This overestimation may be attributed to further reductions of the young water fractions during lateral transport of groundwater to the springs, which is not considered in the model. Where young water fractions are large, overestimations reduce, as the impact of lateral transport is less pronounced. Using a transit time of 60 d to derive the rapid recharge fractions, this overestimation reduces and is replaced by an underestimation of high young water fractions in the Mediterranean region ($r = 0.79$, $P \le 0.001$, *SI Appendix*, Fig. S5). The overall high correlation indicates realistic model behavior and shows that the 60 to 90 d old young water fractions of the carbonate rock springs are most precisely simulated in the ranges larger than ~50% when using the 90 d transit time to derive the rapid recharge fractions, while the 60 d transit time provides better estimates for lower ranges of the young water fractions. A comparison of young water fractions with the simulated rapid recharge fractions obtained by considering diffuse recharge only resulted in substantial underestimations by the model for both the 60 and 90 d transit times (*SI Appendix*, Figs. S3 and S4).

Factors Controlling Rapid Transit to the Groundwater. Focused recharge is the most important driver for the rapid transit of water from the land surface to groundwater. We use our simulation model to quantify the impact of focused recharge and climate on the abundance and strength of rapid transport of pollutants to the groundwater. When considering only diffuse recharge in our model, we find substantially reduced rapid recharge fractions (Mediterranean: $1 \pm 2\%$; mountain: $4 \pm 9\%$; desert: $0 \pm 0.2\%$; humid: $0 \pm 0.7\%$ of rapid recharge compared to total recharge), indicating that focused recharge is the dominant mechanism for rapid transit to groundwater (Fig. 2). Including focused recharge in our simulations, we find that rapid recharge fractions most strongly correlate with the aridity index for both Mediterranean and desert regions (Fig. 2 and *SI Appendix*, Fig. S6 and Table S1). The second strongest correlation is between the rapid recharge fractions and the average number of rainfall events per year as well as mean annual precipitation, both closely correlated with the aridity index ($r = 0.65$ and $r = 0.94$, both $P \le 0.001$, for the Mediterranean and desert regions, respectively). Duration of snow cover and high-intensity events show weak correlations to the rapid recharge fractions for both regions, while a negative correlation with moderate strength ($r = -0.43$, $P \le 0.001$) prevails between temperature and the rapid recharge fractions in the Mediterranean region. In humid and mountain regions, we find the strongest correlations of rapid recharge fractions with mean annual temperature and average months with snow cover ($0.44 \le r \le 0.51$ and $-0.39 \le r \le -0.35$, respectively). A moderate correlation exists with the high-intensity events at both regions too ($0.31 \le r \le 0.32$, $P \le 0.001$). Aridity index and mean annual precipitation show weak correlation to the rapid recharge fractions for both regions.

Our simulations indicate that wetness, expressed by increasing values of the aridity index, mean annual precipitation, and mean annual number of rainfall events, are important secondary controls for the strength of rapid recharge fractions in the carbonate rock areas of the Mediterranean and the desert regions. This finding agrees with local studies that have already shown that limited soil storage capacities (29) and the formation of desiccation cracks and stormy periods favor fast infiltration (30, 31). High rainfall intensities, which tend to correlate with increased recharge (32), do not correlate strongly with the rapid recharge fractions; the weak relationship between rainfall intensity and rapid recharge may be due to our use of gridded rainfall inputs (33) that spatially averages local high-intensity rainfall events over a $0.25° \times 0.25°$
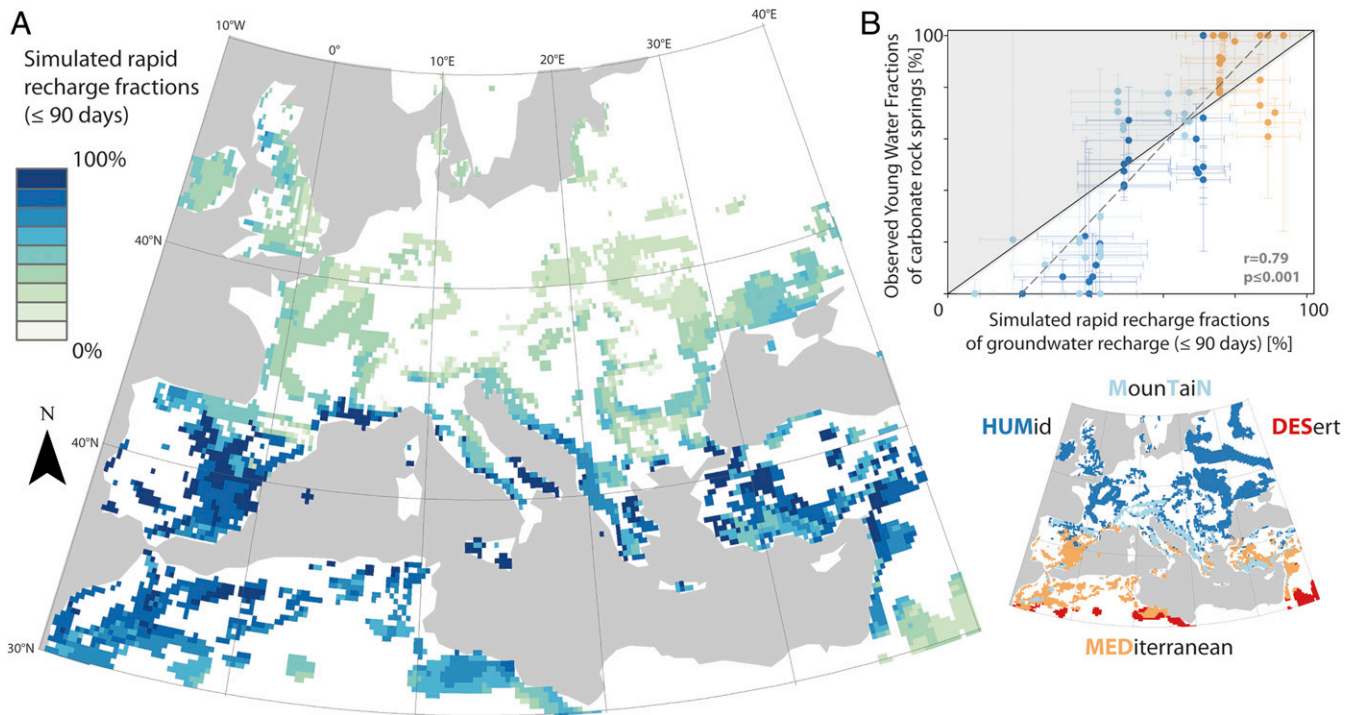
Fig. 1. The simulated rapid recharge fractions of groundwater recharge (%) across the study domain show the highest values in the Mediterranean. A comparison with observed young water fractions of carbonate rock springs indicates realistic model behavior. (*A*) Simulated rapid recharge fractions of groundwater recharge (≤ 90 d; same map with ≤ 60 d in *SI Appendix*, Fig. S5). (*B*) Simulated rapid recharge fractions of groundwater recharge (≤ 90 d) compared to observed young water fractions of the carbonate rock springs across the simulation domain (no observations in the DES region); whiskers indicate SE of simulations and observations; for more details, see *Materials and Methods* and data provided in *SI Appendix*).

grid. While the weak correlations to the duration of snow cover can easily be explained by the lack of substantial snow storage in the Mediterranean and desert regions, the negative correlation with temperature indicates that rapid recharge fractions are reduced by larger losses of infiltrating rainfall to evapotranspiration (14). The positive correlation with the average number of snow months for the humid and mountain regions indicate a reduction of fast recharge through snow storage that may cause a longer delay before the precipitation signal is transmitted to the hydrological system (34). A strong negative correlation between mean annual temperature and average months of snow cover in humid and mountain

regions ($-0.73 \leq r \leq -0.69$, $P \leq 0.001$) demonstrates the influence of temperature on rapid recharge fractions.

Similar results for the four regions are obtained when using 60 d transit times to define the rapid recharge fractions (*SI Appendix*, Fig. S7 and Table S2). Using 25 d transit times, we find a negative correlation between precipitation and the rapid recharge fractions, as well as between aridity index and the rapid recharge fractions, in the humid and mountain regions ($-0.60 \leq r \leq -0.45$, $P \leq 0.001$). Almost none of the other climate descriptors shows linkage to the rapid recharge fractions (*SI Appendix*, Fig. S8 and Table S3). Precipitation is the main control on the value of the aridity
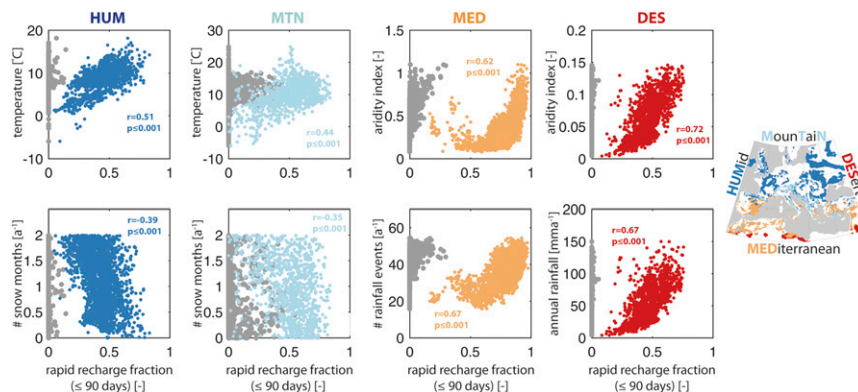
Fig. 2. Scatter plots of the strongest and second strongest correlation of rapid recharge fractions (90 d transit time) and climatic descriptors for the humid (HUM), mountain (MTN), Mediterranean (MED), and desert (DES) regions. Aridity index, the average number of rainfall events, and mean annual precipitation have the strongest control on rapid recharge fractions in the Mediterranean and the desert regions. Gray dots indicate the same relations but with focused recharge not considered. The same figure including all investigated climate variables (25, 60, and 90 d transit times) can be found in the supplement (*SI Appendix*, Figs. S6–S8 and Tables S1–S3).

Hartmann et al.
Risk of groundwater contamination widely underestimated because of fast flow into aquifers

index in humid and mountain regions ($0.80 \leq r \leq 0.91$, $P \leq 0.001$). Its negative correlation with the rapid recharge fractions can be explained by delayed transit through snow storage. A 25 d period may allow for large volumes of precipitation to accumulate as snow but can be too short to include the melting of the snow storage in humid and mountain regions. The Mediterranean region shows similar correlations of climate descriptors and rapid recharge fractions for the 60 and 90 d transit times, while the generally low correlations in the desert region indicate that the time scales of recharge may just be too long compared to the 25 d transit time (35).

Quantification of the Risk of Groundwater Contamination. Fast flow into the groundwater increases the risk of groundwater contamination from pollutants of varying half-lives and survival times, particularly in the Mediterranean region. Our model calculates the rapid recharge fractions corresponding to varying pollutants with half-lives and survival times ranging from 5 to 90 d (Fig. 3). In order to quantify the influence of focused recharge, we repeat the same procedure without considering focused recharge (see model description in *Materials and Methods*). Averaging over all transit times, focused recharge increases the rapid recharge fractions by $20.4 \pm 10.8\%$ (humid region), $24.7 \pm 12.7\%$ (mountain region), $27.7 \pm 10.9\%$ (desert region), and $49.5 \pm 20.5\%$ (Mediterranean), compared to averages of 0.01 to 0.76% when focused recharge is not considered (Fig. 3). Regarding our three example pollutants, we find that $9.9 \pm 8.8\%$ of Salinomycin, $15.5 \pm 13.0\%$ of glyphosate, and $33.1\% \pm 21.5\%$ of *E. coli* remain in groundwater recharge over all simulated carbonate regions when focused recharge is considered (Fig. 3). All three example pollutants show their largest rapid recharge fractions in the Mediterranean region where thin soils, or direct outcrop of bare rocks at the surface, favor rapid fast transit of pollutants to the groundwater.

Using a plausible estimate of 175 mm a^{-1} recharge over our entire simulation domain (18), realistic glyphosate application rates for wheat control of 0.72 to 4.32 kg $ha^{-1} \cdot a^{-1}$ (36), and 50% degradation due to its half-lives of 25 d (22), mean concentrations of 0.32 0.27 µg l^{-1} to 1.91 ± 1.61 µg l^{-1} would still reach groundwater. These simulations show that the maximum permissible concentration of single pesticides in Europe [0.1 µg l^{-1} (37), disregarding metabolites (38)] could be exceeded 3.2 to 19.1 times if focused recharge occurs. Although no comprehensive datasets exist in Europe to evaluate these modeled values, our results correspond well with a national survey conducted in the contiguous United States (27, 28). That study found concentrations of 1.95 ± 1.76 µg l^{-1} in 86 glyphosate detections out of 485 groundwater samples (*SI Appendix*, Fig. S9) collected from carbonate rock aquifers from depths ≤ 20 m, where less dilution and degradation in the groundwater can be expected. Glyphosate was detected ~7.7 times more often within carbonate rock regions, and with median concentrations ~8.4 times higher compared to noncarbonate rock regions (0.65 ± 0.75 µg l^{-1} in 18 detections out of 797 groundwater samples). The large number of nondetections in both datasets can be explained by further degradation in the groundwater, mixing with clean water, or sorption or removal (see *Discussion* below). However, even when considering all nondetections with 0 µg l^{-1}, mean concentrations of 0.34 ± 1.04 µg l^{-1} are found for the 485 groundwater samples taken from carbonate rock aquifers, which is still within range of our simulated concentrations. The nondetections in noncarbonate region results in a mean of 0.01 ± 0.15 µg l^{-1} for the entire set of 797 groundwater samples, which is 23.3 times smaller than the mean concentration found within the carbonate rock regions. These findings correspond well with the results of local studies in Europe, which show that glyphosate detections are generally more likely in karst aquifers in Switzerland (39) and 5.6 times more likely in karst
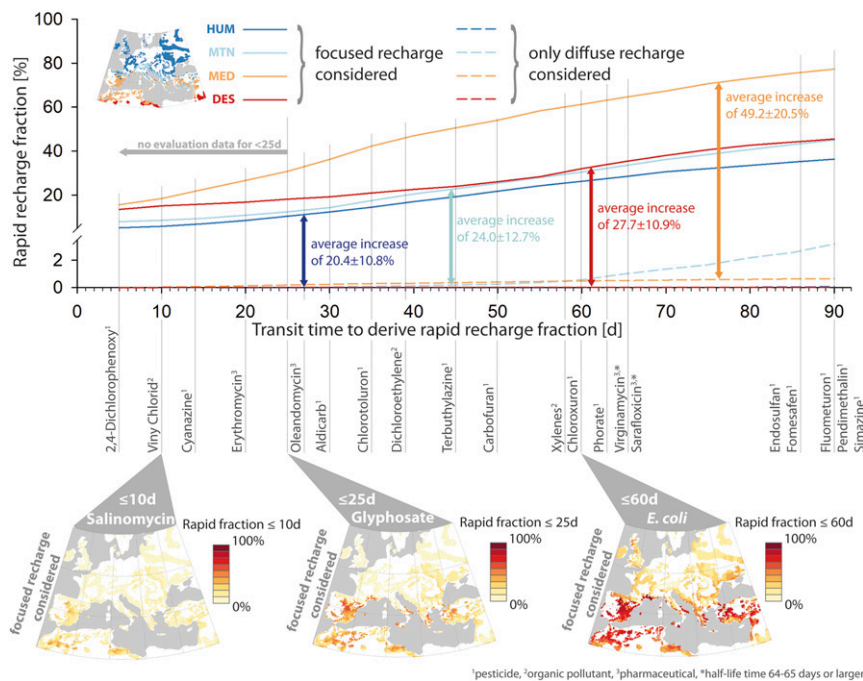
Fig. 3. Rapid recharge fractions of groundwater recharge for transit times of 5 to 90 d for the four simulated regions in relation to 20 example pollutants with varying half-lives (*SI Appendix*, Table S4), and the spatial distribution of the three example pollutants Salinomycin, glyphosate, and *E. coli*. Solid lines represent the simulations including focused recharge processes, while dashed lines indicate the rapid recharge fractions that would occur if only diffuse recharge processes were considered. The simulations are most reliable for transit times between the evaluation with glyphosate observations (25 d) and the evaluation with the Young Water Fractions (60 to 90 d). The error of simulated rapid recharge fractions (one SD) due to model parameter uncertainty is 9, 7, 9, and 14% for the HUM, MTN, MED, and DES regions, respectively. The maps show the spatial distribution of rapid recharge fractions corresponding to the half-lives and survival times of Salinomycin, glyphosate, and *E. coli* when focused recharge is considered.

aquifers compared to fissured nonkarstic aquifers in Ireland (40). Since there is no reason to assume that glyphosate application practices differ between carbonate rock and noncarbonate rock regions, either in Europe nor the United States, this comparison of observed concentrations, with or without nondetections, further supports our finding that focused recharge increases the risk of groundwater contamination.

Discussion

Implications of Potentially Underestimated Contamination. Our carbonate rock recharge estimates only consider vertical infiltration and percolation fluxes. We are aware that infiltrating pollutants may still experience attenuation in transit to the water supply system due to the following: 1) long travel times, as well as dispersion and diffusion processes, especially in deep groundwater systems (our model accounts for depths up to ~30 m); 2) mixing with infiltrating waters from nonpolluted areas from which no contaminants originate; 3) mixing with less polluted groundwater that was recharged before application of the pollutant; 4) sorption to immobile colloids or sediment surfaces in the soil, or 5) removal or retardation of the pollutant during lateral groundwater flow toward a well. While toxicity disappears for most pathogens and pharmaceuticals after removal (11, 12), pesticides can transform into metabolites (38). Furthermore, the half-lives or survival times of all pollutants may strongly vary depending on moisture, temperature, and redox conditions in the unsaturated zone. For all these reasons, and despite their good agreement with observed young water fractions and glyphosate concentrations, our results should be seen as a first-order estimate and worst-case scenarios for the potential risk of contamination in regions with substantial subsurface heterogeneity.

Our continental-scale study highlights that the risk of contamination through focused recharge is not limited to individual sites but relevant across larger scales. Travel times of recharge to the subsurface can be short and tend to be shorter in more arid climates. Thus, fast transit of pollutants to the groundwater poses a significant challenge for water and land use management. The occurrence and likelihood that a contaminant will exceed local regulatory limits are dependent on the pollutant considered, the rate of application, and on permissible concentrations that may vary widely across different countries. Yet, continuing industrial agricultural productivity (13) to optimize food production and feed growing populations (41) will result in increased application of short-lived pollutants to natural systems. Carbonate rock regions cover >20% of Europe's land surface (16) and ~40% of the eastern United States (42). While karstified carbonate rocks can be a valuable source of drinking water (14), we show that increasing agricultural production and population growth may cause substantial and pervasive groundwater pollution. This can result in widespread reduction of available drinking water quality and harm ecosystem services more intensely than previously available large-scale models suggest. While local-scale approaches exist to map and protect areas with increased focused recharge (4), large-scale water quality models are urgently needed to identify regions of increased risk of drinking water contamination over larger scales relevant for water governance (3). Our approach quantifies the risk of groundwater contamination over an entire continent and emphasizes the critical importance of focused groundwater recharge to attempts to predict groundwater pollution.

Materials and Methods

The Carbonate Rock Recharge Model. The model was developed to simulate carbonate rock groundwater recharge over Europe, North Africa, and the Middle East [VarKarst-R (14, 18)]. It simulates terrestrial hydrological processes on a 0.25° × 0.25° grid and at a daily temporal resolution for a 10 y period from 2002 to 2012. Its structure is based on the physical properties and recharge dynamics of the soil and epikarst explored and quantified by previous experimental studies (43–45). Its physical realism and simulation performance was

shown by previous applications at the aquifer scale where high observation densities allowed thorough evaluation (46–48). It includes the spatiotemporal dynamics of diffuse and focused carbonate rock infiltration due to rainfall and snowmelt, evapotranspiration, downward percolation from the upper soil layer to a lower soil epikarst layer (49), and vertical percolation from the epikarst layer toward the groundwater. The latter corresponds to depths up to ~30 m (46), considered in this study as the groundwater depth to which recharge is added. Previous work shows that the model's representation of focused recharge provides more realistic estimates of groundwater recharge in carbonate rock regions compared to other large-scale hydrological models (14, 18) because it assumes that, even within the same hydrological landscape type, there is a distribution of subsurface properties. This variability is considered through distribution functions that allow for variable subsurface storage capacities and vertical hydraulic properties over N horizontally parallel model compartments:

$$S_{max,i} = S_{max,N} \left(\frac{i}{N} \right)^a \qquad [1]$$

$$K_i = K_1 \left(\frac{N - i + 1}{N} \right)^a, \qquad [2]$$

where $S_{max,i}$ (mm) is the subsurface storage capacity of model compartment i; $S_{max,N}$ (mm) is the overall maximum subsurface storage capacity; K_i (d) describes the vertical hydraulic conductivity of the subsurface storage at model compartment i; K_1 (d) is the subsurface storage constant at model compartment 1; and a (-) is a dimensionless shape factor that is related to karstification. In the humid and mountain regions of the modeling domain, a is set to values that favor epikarst and topography-driven interflow processes. In the Mediterranean and desert simulation regions, in combination with thinner soils and less epikarst development, a values favor localized surface runoff toward karstified cracks and fissures that form direct flow paths to the groundwater (see discussion of parameterization in ref. 18).

The N model compartments provide N-simulated time series of groundwater recharge, representing a range of spatially variable recharge dynamics: 1) slow and diffuse recharge at the model compartments with low hydraulic conductivities, 2) lateral redistribution of water from compartments with low hydraulic conductivity to compartments with higher hydraulic conductivity, and 3) fast and focused recharge at those compartments with higher hydraulic conductivity toward which laterally redistributed water is focused.

Within our simulation domain, the model parameters were estimated for four regions, namely humid, mountains, Mediterranean, and deserts, which were identified by climatic and topographic information (18). A large sample of initial model parameter sets (n = 25,000) was created that was iteratively reduced using prior information [e.g., FAO (29)], latent heat flux observations (50) and soil moisture observations (51) for the different regions. The remaining model parameter sets represent the remaining uncertainty of recharge simulations. Their absolute values indicate decreasing soil storages from the humid and mountain regions toward the Mediterranean and deserts regions (18).

When considering diffuse recharge only (Figs. 2 and 3), focused recharge processes are turned off. Instead, infiltrating waters that exceed the vertical percolation capacity of diffuse recharge leave the system as surface runoff that does not contribute to groundwater recharge. Such generation of surface runoff is a typical part of presently available large-scale simulation models [e.g., PCR-GLOBWB (52)]. That way, only diffuse recharge fluxes are simulated in the model without the need to introduce new model parameters. The karst model with only diffuse recharge processes simulates lower recharge volumes that are similar to the diffuse recharge–only simulations of presently available large-scale models (14).

Simulation of Transit Times to the Groundwater. In order to estimate the simulated rapid recharge fractions corresponding to the half-lives and survival times of different pollutants, we first derived simulated transit time distributions from the model's groundwater recharge simulations using virtual tracer experiments. For each hydrological year of the N-simulated time series of groundwater recharge, a virtual tracer is applied to each grid cell's precipitation. Evaluation of the model with observed artificial tracer breakthrough curves (48) and transit times (53) at the catchment scale demonstrates that this representation of transport by mixing assumptions provides a realistic approximation of advection and dispersion processes in carbonate rock systems. The time when the simulated recharge reaches 50% of the input concentration of the tracer is assumed to approximate the mean transit time. By doing so for N-simulated recharge time series (see above), a distribution of mean transit times can be derived. Using the evaluated transit time distribution, we can define transit times that correspond to the half-lives and survival times of selected pollutants and derive the corresponding fraction of simulated

Hartmann et al.
Risk of groundwater contamination widely underestimated because of fast flow into aquifers

groundwater recharge (i.e., the focused and rapid fraction of groundwater recharge that still contains the selected pollutants).

To evaluate the simulated transit time distributions, we use 119 time series of observed water isotope dynamics of carbonate rock springs that we collected over the humid, Mediterranean, mountain, and desert regions. As applied in preceding research (23, 24), we use the ratio of seasonal amplitudes of the water isotope composition of precipitation and spring discharge to estimate the young water fraction (the fraction of spring discharge that is less than 60 to 90 d old). Specifically, we fit a cycle via multiple regression analyses (sinusoidal function) with a frequency of 1 y^{-1} to capture seasonal fluctuations in $\delta^{18}O$ values. The amplitude of the cycle in carbonate rock springs was derived by fitting sine functions to the measured isotope composition time series for each of the 119 springs. Next, we compared spring water seasonal cycle amplitudes against the amplitude of the cycle capturing seasonal variations in precipitation isotope compositions (precipitation isotope amplitudes from ref. 54). The young water fraction is then obtained by the ratio of the spring water $\delta^{18}O$ cycle amplitude and the precipitation $\delta^{18}O$ cycle amplitude (see ref. 23). For realistic estimates, we 1) do not allow young water fractions <0% and >100%, 2) discard those with a coefficient of determination of fitted sine curve and observations $\leq$ 0, and 3) remove those with more than 2 mo of continuous snow cover, creating substantial delay before infiltration. This resulted in 78 reliable estimates of young water fractions for our evaluation.

A preliminary comparison of observed young water fractions of the nondiscarded springs (78 in total; see *SI Appendix*, Tables S5 and S6) with the simulated rapid recharge fractions that are younger than 90 d (derived from the simulated transit time distributions) shows that the observed young water fractions have to be corrected for seasonality of rainfall, which is already known to produce bias in young water fraction estimation (25). In our dataset, this bias is expressed as a strong correlation of rainfall seasonality (ratio of average precipitation in July, August, and September, and an average precipitation in January, February, and March), with the deviation between simulated rapid recharge fractions and observed young water fractions (*SI Appendix*, Fig. S1). We use this correlation to obtain seasonality corrected estimates of observed young water fractions (Fig. 1B). Uncertainty of the observed young water fractions is expressed by the combined SEs of the amplitude estimates of the rainfall and carbonate rock spring isotopic signals derived by Gaussian error propagation. Uncertainty of the simulated rapid recharge fractions represents the remaining uncertainty (one SD) after parameter estimation of the continental recharge model (see above). Since

the observed young water fractions are only defined within a range (60 to 90 d), we repeat the same procedure with a transit time of 60 d to derive the rapid recharge fractions (*SI Appendix*, Figs. S2 and S5B).

Derivation of Climatic Controls. To explore the impact of climate on rapid recharge fractions, we derive different climate descriptors from the daily 10 y input data of the continental carbonate rock recharge model (18): mean annual precipitation, mean annual temperature, aridity index (defined as mean annual precipitation over potential evapotranspiration), mean annual number of rainfall events (defined as time periods with $\geq$ 1 mm of daily rainfall), mean annual number of months with snow cover, and high-intensity rainfall events defined by the mean intensity of the upper quartile of rainfall events. We explore the linkage between these climatic controls and rapid recharge fractions using the 90 d transit time, which corresponds to a seasonal time scale, because the model evaluation was performed using the same transit time (*SI Appendix*, Table S1 and Fig. S6 and Fig. 2). The same procedure is repeated using the alternate transit times for the model evaluation (60 d; see *SI Appendix*, Table S2 and Fig. S7; 25 d; see *SI Appendix*, Table S3 and Fig. S8). Correlations are quantified through their Pearson correlation coefficients r and their significance p (using a significance level alpha of 0.05). We use r instead of r^2 to be able to distinguish positive and negative relationships.

Data Availability. The code of the carbonate rock recharge model is available at https://github.com/KarstHub/VarKarst-R-2015. The time series of stable isotopes ($\delta^{18}O$) of the 78 carbonate rock springs are available for download at https://doi.org/10.6084/m9.figshare.13020365. The raw data of the glyphosate concentrations in groundwater is freely available at https://www.waterqualitydata.us. All other study data are included in the article and/or *SI Appendix*.

1. N. Hofstra, C. Kroeze, M. Flörke, M. T. van Vliet, Editorial overview: Water quality: A new challenge for global scale model development and application. *Curr. Opin. Environ. Sustain.* **36**, A1–A5 (2019).
2. A. Y. Hoekstra, M. M. Mekonnen, The water footprint of humanity. *Proc. Natl. Acad. Sci. U.S.A.* **109**, 3232–3237 (2012).
3. M. T. H. Van Vliet, M. Florke, Y. Wada, Quality matters for water scarcity. *Nat. Geosci.* **10**, 800–802 (2017).
4. D. Daly et al., Main concepts of the "European approach" to karst-groundwater-vulnerability assessment and mapping. *Hydrogeol. J.* **10**, 340–345 (2002).
5. B. Andreo et al., Karst groundwater protection: First application of a Pan-European approach to vulnerability, hazard and risk mapping in the Sierra de Líbar (Southern Spain). *Sci. Total Environ.* **357**, 54–73 (2006).
6. W. B. White, *Geomorphology and Hydrology of Karst Terrains* (Oxford University Press, 1988), vol. 1.
7. D. Ford, P. Williams, *Karst Hydrogeology and Geomorphology* (John Wiley & Sons Ltd, 2007).
8. S. R. H. Worthington, G. J. Davies, E. C. Alexander, Enhancement of bedrock permeability by weathering. *Earth Sci. Rev.* **160**, 188–202 (2016).
9. N. J. Jarvis, A review of non-equilibrium water flow and solute transport in soil macropores: Principles, controlling factors and consequences for water quality. *Eur. J. Soil Sci.* **58**, 523–546 (2007).
10. M. J. Ascott et al., Global patterns of nitrate storage in the vadose zone. *Nat. Commun.* **8**, 1416 (2017).
11. K. Kümmerer, *Pharmaceuticals in the Environment: Sources, Fate, Effects and Risks* (Springer Science & Business Media, 2008).
12. WHO, "Section II: Understanding the drinking-water catchment" in *Protecting Groundwater for Health: Managing the Quality of Drinking-Water Sources*, O. Schmoll, G. Howard, J. Chilton, I. Chorus, Eds. (World Health Organization, 2006).
13. J. A. Foley et al., Solutions for a cultivated planet. *Nature* **478**, 337–342 (2011).
14. A. Hartmann, T. Gleeson, Y. Wada, T. Wagener, Enhanced groundwater recharge rates and altered recharge sensitivity to climate variability through subsurface heterogeneity. *Proc. Natl. Acad. Sci. U.S.A.* **114**, 2842–2847 (2017).
15. Z. Stevanović, Karst waters in potable water supply: A global scale overview. *Environ. Earth Sci.* **78**, 1–12 (2019).
16. N. Goldscheider et al., Global distribution of carbonate rocks and karst water resources. *Hydrogeol. J.* **28**, 1661–1677 (2020).
17. N. Goldscheider, D. Drew, *Methods in Karst Hydrogeology* (Taylor & Francis Ltd, 2007).
18. A. Hartmann et al., A large-scale simulation model to assess karstic groundwater recharge over Europe and the Mediterranean. *Geosci. Model Dev.* **8**, 1729–1746 (2015).
19. W. B. White et al., *Karst Groundwater Contamination and Public Health* (Springer, 2016).
20. B. R. Scanlon, W. R. Healy, P. G. Cook, Choosing appropriate techniques for quantifying groundwater recharge. *Hydrogeol. J.* **10**, 18–39 (2002).
21. A. Hartmann, VarKarst-R-2015. GitHub. https://github.com/KarstHub/VarKarst-R-2015 (Accessed 22 April 2021).
22. K. A. Lewis et al., Human and Ecological Risk Assessment: An International an international database for pesticide risk assessments and management and management. *Hum. Ecol. Risk Assess.* **22**, 1050–1064 (2016).
23. J. W. Kirchner, Aggregation in environmental systems-Part 1: Seasonal tracer cycles quantify young water fractions, but not mean transit times, in spatially heterogeneous catchments. *Hydrol. Earth Syst. Sci.* **20**, 279–297 (2016).
24. S. Jasechko, J. W. Kirchner, J. M. Welker, J. J. McDonnell, Substantial proportion of global streamflow less than three months old. *Nat. Geosci.* **9**, 126–129 (2016).
25. J. W. Kirchner, Aggregation in environmental systems-Part 2: Catchment mean transit times and young water fractions under hydrologic nonstationarity. *Hydrol. Earth Syst. Sci.* **20**, 299–328 (2016).
26. A. Hartmann, Isotope Data. *Figshare*. https://figshare.com/articles/dataset/Isotope_data_zip/13020365 (Accessed 22 April 2021).
27. E. A. Scribner, W. A. Battaglin, R. J. Gilliom, M. T. Meyer, *Concentrations of Glyphosate, Its Degradation Product, Aminomethylphosphonic Acid, and Glufosinate in Ground- and Surface-Water, Rainfall, and Soil Samples Collected in the United States, 2001–06* (U.S. Geological Survey, 2007). Sci. Investig. Rep. **2007–5122**.
28. E. K. Read et al., Water quality data for national-scale aquatic research: The Water Quality Portal. *Water Resour. Res.* **53**, 1735–1745 (2017).
29. P. A. Sanchez, Digital soil map of the world. *Science* **325**, 680–681 (2009).
30. J. F. Martínez-Murillo, E. Nadal-Romero, D. Regüés, A. Cerdà, J. Poesen, Soil erosion and hydrology of the western Mediterranean badlands throughout rainfall simulation experiments: A review. *Catena* **106**, 101–112 (2013).
31. B. Andreo et al., Influence of rainfall quantity on the isotopic composition (18O and 2H) of water in mountainous areas. Application for groundwater research in the Yunquera-Nieves karst aquifers (S Spain). *Appl. Geochem.* **19**, 561–574 (2004).
32. V. Allocca, P. De Vita, F. Manna, J. R. Nimmo, Groundwater recharge assessment at local and episodic scale in a soil mantled perched karst aquifer in southern Italy. *J. Hydrol. (Amst.)* **529**, 843–853 (2015).

6 of 7 | PNAS
https://doi.org/10.1073/pnas.2024492118

Hartmann et al.
Risk of groundwater contamination widely underestimated because of fast flow into aquifers

33. B. Y. M. Rodell *et al.*, The global land data Assimilation system. *Bull. Am. Meteorol. Soc.* **85**, 381–394 (2004).

34. M. Paul Stockinger, H. Reemt Bogena, A. Lücke, C. Stumpp, H. Vereecken, Time variability and uncertainty in the fraction of young water in a small headwater catchment. *Hydrol. Earth Syst. Sci.* **23**, 4333–4347 (2019).

35. J. J. de Vries, I. Simmers, Groundwater recharge: An overview of process and challenges. *Hydrogeol. J.* **10**, 5–17 (2002).

36. European Food Safety Authority (EFSA), Peer review of the pesticide risk assessment of the potential endocrine disrupting properties of glyphosate. *EFSA J.* **15**, e04979 (2017).

37. EC, Council Directive 98/83/EC of 3 November 1998 on the quality of water intended for human consumption. *Off. J. Eur. Communities.* **41**, 32–54 (1998).

38. C. N. Sawyer, P. L. McCarty, G. F. Parkin, *Chemistry for Environmental Engineers* (McGraw-Hill Education, ed. 5, 2002).

39. T. Poiger, I. J. Buerge, A. Bächli, M. D. Müller, M. E. Balmer, Occurrence of the herbicide glyphosate and its metabolite AMPA in surface waters in Switzerland determined with on-line solid phase extraction LC-MS/MS. *Environ. Sci. Pollut. Res. Int.* **24**, 1588–1596 (2017).

40. S. L. McManus, K. G. Richards, J. Grant, A. Mannix, C. E. Coxon, Pesticide occurrence in groundwater and the physical characteristics in association with these detections in Ireland. *Environ. Monit. Assess.* **186**, 7819–7836 (2014).

41. FAO and IWMI, "More people, more food, worse water? A global review of water pollution from agriculture", 978-92-5-130729-8 (FAO) (Food and Agriculture Organization of the United Nations Rome and the International Water Management Institute on behalf of the Water Land and Ecosystems research program of the CGIAR Colombo, 2018).

42. W. B. White, D. C. Culver, J. S. Herman, T. C. Kane, J. E. Mylroie, Karst lands. *Am. Sci.* **83**, 450–459 (1995).

43. P. W. Williams, The role of the subcutaneous zone in karst hydrology. *J. Hydrol. (Amst.)* **61**, 45–67 (1983).

44. J. Lange, Y. Arbel, T. Grodek, N. Greenbaum, Water percolation process studies in a Mediterranean karst area. *Hydrol. Processes* **24**, 1866–1879 (2010).

45. L. Aquilina, B. Ladouche, N. Dörfliger, Water storage and transfer in the epikarst of karstic systems during high flow periods. *J. Hydrol. (Amst.)* **327**, 472–485 (2006).

46. A. Hartmann, J. Lange, M. Weiler, Y. Arbel, N. Greenbaum, A new approach to model the spatial and temporal variability of recharge to karst aquifers. *Hydrol. Earth Syst. Sci.* **16**, 2219–2231 (2012).

47. A. Hartmann, J. A. Barberá, J. Lange, B. Andreo, M. Weiler, Progress in the hydrologic simulation of time variant recharge areas of karst systems–Exemplified at a karst spring in Southern Spain. *Adv. Water Resour.* **54**, 149–160 (2013).

48. M. Mudarra, A. Hartmann, B. Andreo, Combining experimental methods and modeling to quantify the complex recharge behavior of karst aquifers. *Water Resour. Res.* **55**, 1384–1404 (2019).

49. P. W. Williams, The role of the epikarst in karst and cave hydrogeology: A review. *Int. J. Speleol.* **37**, 1–10 (2008).

50. D. Baldocchi *et al.*, FLUXNET: A new tool to study the temporal and spatial variability of ecosystem–Scale carbon dioxide, water vapor, and energy flux densities. *Bull. Am. Meteorol. Soc.* **82**, 2415–2434 (2001).

51. W. A. Dorigo *et al.*, The international soil moisture network: A data hosting facility for global in situ soil moisture measurements. *Hydrol. Earth Syst. Sci.* **15**, 1675–1698 (2011).

52. Y. Wada, D. Wisser, M. F. P. Bierkens, Global modeling of withdrawal, allocation and consumptive use of surface water and groundwater resources. *Earth Syst. Dyn.* **5**, 15–40 (2014).

53. A. Hartmann *et al.*, Model-aided quantification of dissolved carbon and nitrogen release after windthrow disturbance in an Austrian karst system. *Biogeosciences* **13**, 159–174 (2016).

54. S. T. Allen *et al.*, Global sinusoidal seasonality in precipitation isotopes. *Hydrol. Earth Syst. Sci. Discuss.* **23**, 3423–3436 (2019).

ENVIRONMENTAL SCIENCES

SUSTAINABILITY SCIENCE